Fluorescence Anisotropy Decay Studies of Local Polymer Dynamics in the Melt. 1. Labeled Polybutadiene

Jean-Louis Viovy* and Lucien Monnerie

Laboratoire de Physicochimie Structurale et Macromolêculaire, E.S.P.C.I., 75231 Paris Cedex 05, France

Fabienne Merola

Laboratoire pour l'Utilisation du Rayonnement Electromagnêtique, Universitê Paris-Sud et CNRS, 91401 Orsay Cedex, France. *Received January 27, 1984*

ABSTRACT: The fluorescence anisotropy decay of polybutadiene labeled with anthracene in the middle of the chain and embedded in a matrix of unlabeled polybutadiene is studied in the temperature range −50 to +80 °C. Very good precision is achieved thanks to the use of synchrotron radiation as the exciting source. The anisotropy is compared to different phenomenological expressions and molecular models proposed in the literature, using a multicriteria evaluation procedure. Intramolecular connectivity is shown to play an essential role in orientational dynamics in the melt. We also show that rather local orientational motions follow the same temperature law as macroscopic mechanical properties.

Introduction

Polymer orientational dynamics in solution are now rather well described by molecular models taking into account the connectivity of the chains.[1-5] But polymer dynamics in the melt are less well-known. Several reasons can be put forward to explain this poorer knowledge. From a technical point of view, the relaxation times are generally longer in melts than in solutions, so that molecular spectroscopic techniques are more difficult to apply. From a fundamental point of view, chain dynamics and viscosity are a unique phenomenon, including intramolecular and intermolecular interactions. Fundamental questions such as the importance of conformational changes or the scale of "elementary motions" and "cooperative regions" are still poorly understood.

Polymer melts were first studied extensively by mechanical[6] and dielectric[7] relaxations. These techniques brought out several striking phenomenological properties of polymer materials, such as the critical slowing down of dynamics when the temperature is lowered, the existence of a glass transition and of secondary relaxations, the time–temperature superposition equation, and the wide distributions of relaxation times in the spectra. The molecular interpretation of these kinds of experiments is difficult since they are sensitive to cross-correlation functions including monomers of different chains. More recently, spectroscopic methods exploring the orientation autocorrelation function (OACF) of a given vector in the chain, such as NMR,[8-10] ESR,[1] or fluorescence polarization under continuous excitation,[12] were applied to polymer melts. Numerous local processes were observed in this way and interpreted in terms of primary and secondary relaxations. But, to our knowledge, the rare attempts to take into account the nonexponential character of the OACF were based on the phenomenological Williams–Watts (WW) distribution,[13] with relatively little benefit to our knowledge of molecular processes.

In a recent paper,[5] we used fluorescence anisotropy decay (FAD) to discuss the different models proposed in the literature for polymer orientational dynamics in solution. Experimental evidence ruled out several models, in particular the Williams–Watts expression. One can thus wonder if the molecular models suitable for polymer solutions account for polymer dynamics in the melt also, or if these materials possess specific autocorrelation functions.

The purpose of this series is to present several studies of polymer dynamics in the melt by FAD. In the present paper, we investigate the dynamics of a polybutadiene chain labeled with anthracene in the middle of the chain (PBAPB) embedded in a matrix of identical but unlabeled chains (PB).

Methods and Technique

Dynamical Studies Using Fluorescence Anisotropy Decay (FAD). Fluorescent species are able to absorb photons at a certain wavelength (most often in the UV range) and reemit them later at a higher wavelength. Excitation of a medium containing fluorescent molecules by a short-duration pulse of light is followed by an emission of fluorescence light. The decay of fluorescence intensity is roughly exponential, and the fluorescence lifetime is generally in the nanosecond range.

The absorption of light by a molecule is proportional to the scalar product of the incident electric field and of a molecular vector called the absorption transition moment. Thus, excitation of an isotropic fluorescent medium by polarized light generally creates a temporary anisotropic population of excited molecules. Molecular motions progressively destroy this anisotropy and affect the polarization of fluorescence light.

In a usual FAD experiment, the medium is excited by a nanosecond pulse of vertically polarized light. The emitted fluorescence is recorded as a function of time in both vertical (parallel) and horizontal (perpendicular) polarizations. When the emission and absorption moments are parallel, the emission anisotropy

$$r(t) = [I_V(t) - I_H(t)]/[I_V(t) + 2I_H(t)] \quad (1)$$

is proportional to the second moment of the OACF of the transition moment

$$r(t) = r_0 M_2(t)/M_2(0) \quad (2)$$

where

$$M_2(t) = \tfrac{1}{2}\langle 3[\cos(\mu(0),\mu(t))]^2 - 1\rangle$$

$(\mu(0),\mu(t))$ is the angle between the positions of the transition moment at time 0 and at time t.

The fundamental anisotropy r_0 is a molecular parameter related to electronic delocalization. r_0 is independent of time and it can take values between −0.2 and +0.4. Thus, the OACF $M_2(t)$ can be sampled quasi-continuously directly in the time domain. This property makes FAD suitable to study the main orientation decorrelation processes. On the other hand, because of the exponential nature of fluorescence decay, the precision is lower at long times, and this technique is poorly adapted to study the evolution of residual orientations. Values of the OACF lower than, say, 0.05 cannot be measured precisely.

Fluorescent Labeling of a Polymer Chain. To study the dynamics of polymer chains, an anthracene group is covalently

0024-9297/85/2218-1130$01.50/0

Table I
Characteristics of the Polybutadienes Used in the Present Study

symbol	nature	T_g,[a] °C	microstructure % cis	% trans	% 1-2	$10^{-5}M_n$	$10^{-5}M_w$
PB	unlabeled	-90	37	51	12	1.7	4.1
PBA	labeled	-90	37	51	12	1.86	

[a] DSC.

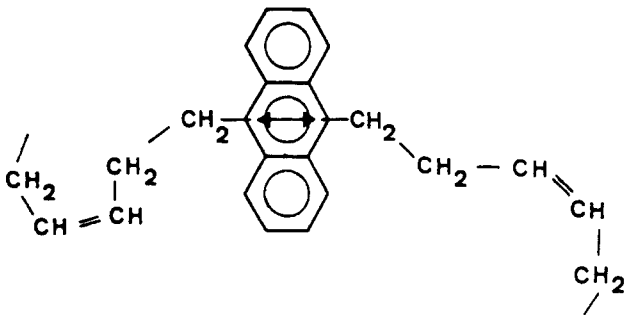

Figure 1. Polybutadiene labeled with anthracene in the middle of the chain.

coupled in the middle of the chain with its emission and first absorption moments tangent to the skeleton (Figure 1), following the method developed by Valeur and co-workers.[14] To check if this dye really reflects polymer dynamics, we performed a separate experiment, using noncoupled 1,9-dimethylanthracene in the same PB matrix. The motion of the noncoupled dye was always two decades or more faster than that of the coupled one. Thus, in the labeled chain, the inertia or friction of the dye is negligible as regards intrachain constraints. Since the dye is rigid and bonded in the 1,9-positions, its own rotation around the 1,9-axis has no action on the OACF. Of course, the dye modifies locally the conformational properties (geometry and energy) of the chain, so that FAD is certainly not the best tool to study quantitatively relaxation times of a given polymer. However, at the present level of understanding, it is a rather unique technique to answer several general questions about the dynamics of linear, flexible chains.

Fluorescence Anisotropy Equipment. The experiments were performed on the cyclosynchrotron LURE-ACO at Orsay (France). The apparatus is described elsewhere.[15] The continuous spectrum from the synchrotron allowed for the matching of the last absorption peak of the dye (401 nm). This excitation wavelength was selected by a double holographic grating with 2-nm slits, and the most intense emission peak (435 nm) was selected by a single holographic grating with 2-nm slits. This procedure greatly improves the rejection of spurious fluorescence, which is one of the major problems of fluorescence studies in bulk polymers. The negligible level of spurious fluorescence was checked by using blank samples of the unlabeled matrix. The transmission of the emission monochromator was calibrated in both polarizations with a 0.005 precision.

The polarized emission spectra and the apparatus response (recorded at emission wavelength) were sampled with a 0.12-ns channel width by the single-photon counting technique. Thanks to the stability of the pulses, the short-time limit of the experimental window is about 0.1 ns. The upper limit, imposed by the repetition rate of the pulses and the lifetime of the dye, is 62 ns.

Cell and Sample Separation. Even above the glass transition, high molecular weight elastomers are too viscous to be introduced into standard cells. On the other hand, films prepared with these materials have a poor surface quality and cannot retain a precise shape and thickness over long periods of time. Cross-linking improves the mechanical properties, but not the surface state, and introduces extra fluorescence.

To overcome these difficulties, we used a cell specially devised for elastomers. A horizontal cross section of this cell is shown schematically in Figure 2. Two asymmetric quartz prisms hold the film under study. The vertically polarized exciting beam crosses the interfaces air–quartz (A) and quartz–polymer (B) without any perturbation of its polarization. The light reflected in B does not enter the collecting diaphragm at interface D. The rough polymer–air interface (F) is not illuminated. The transmission of interface for both polarizations can be corrected by using the laws of refraction

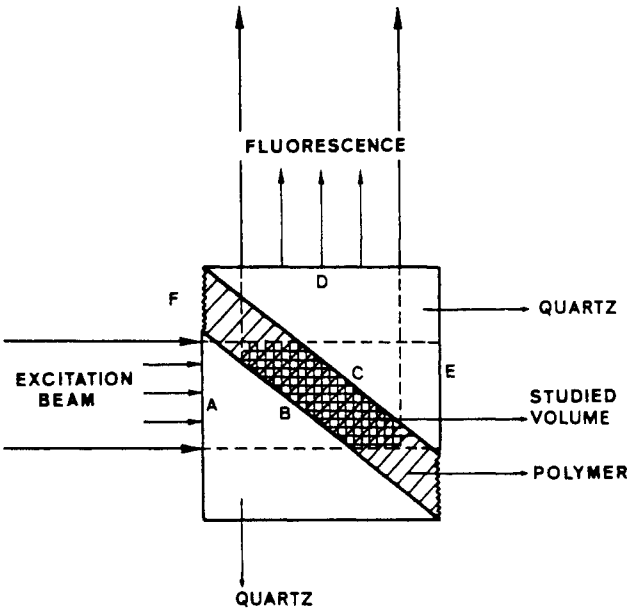

Figure 2. Cross section of the fluorescence cell for high molecular weight polymer melts.

$$\tau_H/\tau_V = \frac{1 - [tq^2(i-\alpha)/tg^2(i+\alpha)]}{1 - [\sin^2(i-\alpha)/\sin^2(i+\alpha)]} \quad (3)$$

with $i = \arcsin(\sin(\alpha) n_q/n_p)$. τ_H and τ_V are the transmitivities for horizontally and vertically polarized light, α is the smaller angle of the prism (see Figure 2), and n_q and n_p are the refractive indexes of quartz and of the polymer at the emission wavelength. For polybutadiene, this correction is lower than 10^{-3}.

The samples of labeled and unlabeled polybutadiene were provided by the Michelin Co. Their characteristics are quoted in Table I. They were purified by extraction with acetone. Then, films of un-cross-linked polybutadiene (PB) containing a small amount of labeled chains (PBAPB) were cast from toluene solutions. The optical density of the films was less than 0.1 to avoid energy transfer and reabsorption. The polymer films were placed into the cell by a sequence of molding and stoving operations in an argon atmosphere to avoid bubbles, ensure perfect adhesion at the interfaces, and relax stresses.

Data Fitting Procedure and Evaluation Criteria. The discussion of nonisotropic motions observed in a spectroscopic experiment requires some criteria adapted to the technique being used and a systematic method to apply them. We developed in ref 5 such a method for FAD.

In a single-photon fluorescence decay experiment, the major error in the data is Poisson noise. The knowledge of the statistics of the data allows automatic computer fitting procedures for any parameterized model and provides objective statistical criteria. The most well-known of these criteria is the reduced mean square deviation χ^2:

$$\chi^2 = \frac{1}{N}\sum_{i=1}^{N}\frac{(U_i - u_i)^2}{U_i} \quad (4)$$

N is the number of channels and U_i the experimental value in channel i. u_i is the best-fit computed value for channel i. The mean expected value χ^2 is 1 for a "perfect" model and no sys-

Table II
Expressions for the OACF Used throughout the Paper

ref	abbrevn	expression
13	WW	$r(t) = r_0 \exp((-t/\tau)\beta)$
1	VJGM	$r(t) = r_0 \exp((1/\tau_1 - 1/\tau_2)t)$ erfc $((t/\tau_1)^{1/2})$
2	JS	$r(t) = r_0 \sum_{i=1}^{n} a_i \exp(-t/\tau_i)$ (The values for τ_i and a_i are tabulated in ref 2.)
3	BY	$r(t) = 0.5 r_0 (\pi/t)^{1/2} (\tau_2^{-1/2} - \tau_1^{-1/2})$(erfc $((t/\tau_1)^{1/2}$ - erfc $((t/\tau_2)^{1/2})$)
4	HH	$r(t) = r_0 \exp(-t/\tau_2) \exp(-t/\tau_1) I_0(t/\tau_1)$
19	RR	$r(t) = r_0((1 - \beta) \exp(-t/\tau_1) + \beta)$
5	GDL	$r(t) = r_0 \exp(-t/\tau_2 - t/\tau_1)(I_0(t/\tau_1) + I_1(t/\tau_1))$

tematic error. For a given data set and different models, the lower χ^2 is, the better the model is.

But other statistical information exists. The variance–covariance matrix indicates if a fitted parameter is statistically significant or not,[16] and how many free parameters can be fitted reasonably to a given data set. By plotting the weighted residuals as a function of channel number, one can judge by visual observation the nature of the deviations between the model and the experiment. Finally, different experimental artifacts like nonrandom oscillations can be detected by more sophisticated quantities such as the autocorrelation of residuals[17] or the Durbin and Watson parameter.[18]

But the physical meaning of a model cannot be assessed by fitting criteria alone. One must also ensure that the fitted values of the parameters are consistent with the hypotheses of the underlying model. For example, the fundamental anisotropy r_0, which is an adjustable parameter in all the models discussed below, must take values between −0.2 and +0.4 for theoretical reasons. In the present set of experiments, the value of r_0 even provides a more severe criterion, since it is related to the respective fluctuations of the emission and absorption moments which are only weakly perturbed by the PB chains covalently bonded to the anthracene group. Thus, the values of r_0 must not differ much from those obtained for dimethylanthracene (DMA) under the same conditions and in the same matrix. A separation experiment performed on DMA in a PB matrix permits the reduction of the reasonable range for r_0 to 0.1–0.3.

Besides these absolute limits, if a model is supposed to reflect the true OACF on the whole experimental window, the best-fit parameters should not change when only a part of the data is used. Thus, for a given data set, best-fit parameters should be relatively stable with respect to variations in the fitting window (small variations cannot be avoided because of the statistical nature of the data). To check this, we fitted all the models to five differently truncated portions of the same experimental data set and studied the variation of the best-fit parameters from one fit to the other.

Of course, none of the aforementioned criteria can prove that a model is the unique realistic representation of molecular motions. But they seen already very useful to draw distinctions between the numerous expressions proposed in the literature.

Results

Discussion of Models. We recorded the fluorescence

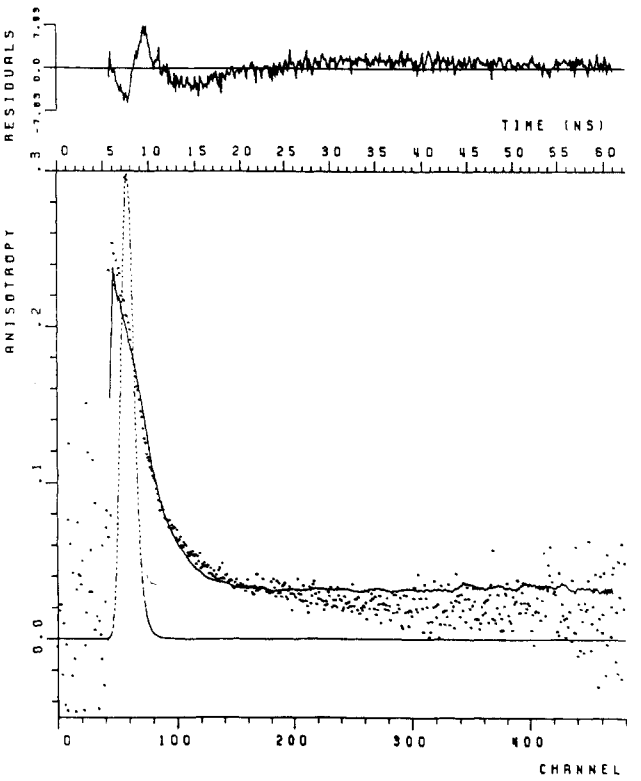

Figure 3. Comparison of the restricted rotation model to the experimental anisotropy at 62.7 °C. Dots are experimental data. The continuous line is the best-fit OACF reconvoluted by the measured instrumental function (exciting pulse). This pulse is plotted as a dash–dot line (arbitrarily scaled). The upper graph represents the weighted residuals.

anisotropy of PBAPB in the range −50 to +80 °C. Below +50 °C, only a part of the OACF is in the experimental window. Thus, we focus here on the results obtained in the range 50–80 °C, where the OACF is sampled almost completely. In that way, only small residual anisotropies are discarded, and the discussion of the main relaxation processes remains unambiguous. The expressions used in this present paper are gathered in Table II.

Their physical basis was discussed in some detail in ref 5 and shall be recalled briefly only when necessary. For more details, the reader is invited to refer to ref 5 or to the original papers.

The best-fit parameters for the different models at 62.7 and 80 °C are gathered in Tables III–V. Some best-fit decays are compared to the corresponding data set (62.7 °C) in Figures 3–7. The dots represent experimental points, the continuous line the reconvoluted best fit, and

Table III
Best-Fit Parameters for Models VJGM and WW

	80 °C					62.7 °C				
truncation[a]	χ^2	r_0	τ_1, ns	τ_2,[b] ns	τ_2/τ_1	χ^2	r_0	τ_1, ns	τ_2,[b] ns	τ_1/τ_2
				VJGM Model						
1	1.0622	0.374	0.390	11.88	30.5	1.9709	0.336	1.07	30.6	28.6
2	1.011	0.387	0.362	11.6	32.2	1.774	0.345	0.99	31.5	31.8
3	0.96936	0.375	0.370	12.1	32.7	1.134	0.424	0.60	29.1	48.5
4	1.1164	0.373	0.395	11.8	29.9	2.416	0.332	1.13	28.9	25.6
5	1.2567	0.371	0.406	11.3	27.8	2.2754	0.311	1.61	19.5	11.7
				WW Model						
1	1.0677	0.383	0.511	0.370		1.8650	0.333	1.568	0.394	
2	1.0163	0.410	0.422	0.353		1.7213	0.347	1.40	0.381	
3	0.9478	0.628	0.127	0.284		1.299	0.596	0.28	0.275	
4	1.1760	0.383	0.568	0.371		2.200	0.330	1.61	0.400	
5	1.2478	0.371		0.384		2.0017	0.307	1.98	0.446	

[a] 1: 0–55 ns. 2: 1.3–55 ns. 3: 3.2–55 ns. 4: 0–37 ns. 5: 0–17 ns. [b] Or β.

Table IV
Best-Fit Parameters for the JS Model

number of "bonds"	truncation[a]	80 °C			62.7 °C		
		χ^2	r_0	τ, ns	χ^2	r_0	τ, ns
13	1	1.7904	0.345	0.835	2.179	0.278	2.447
	2	1.8108	0.345	0.836	2.171	0.280	2.423
	3	1.4072	0.284	1.0342	2.186	0.282	2.377
	4	2.239	0.345	0.835	2.575	0.280	2.407
	5	2.6018	0.355	0.792	3.6104	0.289	2.223
9	1	2.084	0.281	1.33	2.718	0.254	3.14
	3	1.401	0.214	1.83	2.353	0.228	3.74
	5	3.346	0.286	1.28	1.894	0.267	2.79
5	1	3.23	0.226	2.37	6.650	0.224	4.79

[a] 1: 0–55 ns. 2: 1.3–55 ns. 3: 3.2–55 ns. 4: 0–37 ns. 5: 0–17 ns.

Table V
Best-Fit Parameters for Models HH, GDL, and BY

truncation[a]	80 °C					62.7 °C				
	χ^2	r_0	τ_1, ns	τ_2, ns	τ_2/τ_1	χ^2	r_0	τ_1, ns	τ_2, ns	τ_2/τ_1
				HH Model						
1	0.962	0.246	1.020	22.10	21.6	1.2477	0.234	1.222	96.8	43.6
2	0.9610	0.249	0.985	22.4	22.8	1.233	0.234	2.22	101.1	45.5
3	0.966	0.210	1.35	22.7	16.8	1.1053	0.212	2.73	89.0	32.6
4	1.018	0.248	0.98	22.4	22.7	1.434	0.234	2.23	95.2	42.6
5	1.018	0.248	1.00	21.4	21.5	1.8238	0.234	2.26	83.8	37.1
				GDL Model						
1	0.9779	0.268	0.332	11.9	35.8	1.176	0.251	0.753	35.9	47.7
2	0.9759	0.270	0.326	11.9	36.5	1.149	0.253	0.745	35.9	48.2
3	0.9610	0.238	0.404	13.3	32.9	1.120	0.265	0.67	34.4	51.3
4	1.039	0.168	0.332	11.9	35.4	1.320	0.251	0.76	35.3	46.4
5	1.023	0.267	0.336	11.6	34.5	1.400	0.247	0.82	30.4	37.0
				BY Model						
1	0.9503	0.259	0.282	38.9	137	1.1917	0.242	0.641	151	235
2	0.9488	0.261	0.278	39.3	141	1.1773	0.242	0.638	152	238
3	0.9562	0.242	0.320	38.9	122	1.168	0.230	0.718	139	193
4	1.0028	0.259	0.282	38.7	136	1.327	0.242	0.647	144	222
5	0.9817	0.257	0.291	36.6	125	1.4664	0.240	0.681	112	164

[a] 1: 0–55 ns. 2: 1.3–55 ns. 3: 3.2–55 ns. 4: 0–37 ns. 5: 0–17 ns.

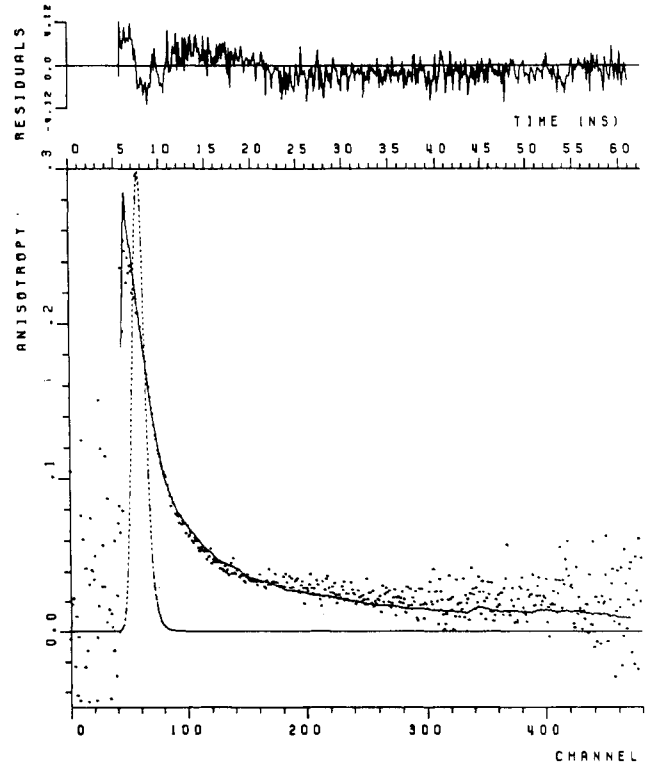

Figure 4. Comparison of Williams and Watts' expression to the experimental anisotropy at 62.7 °C.

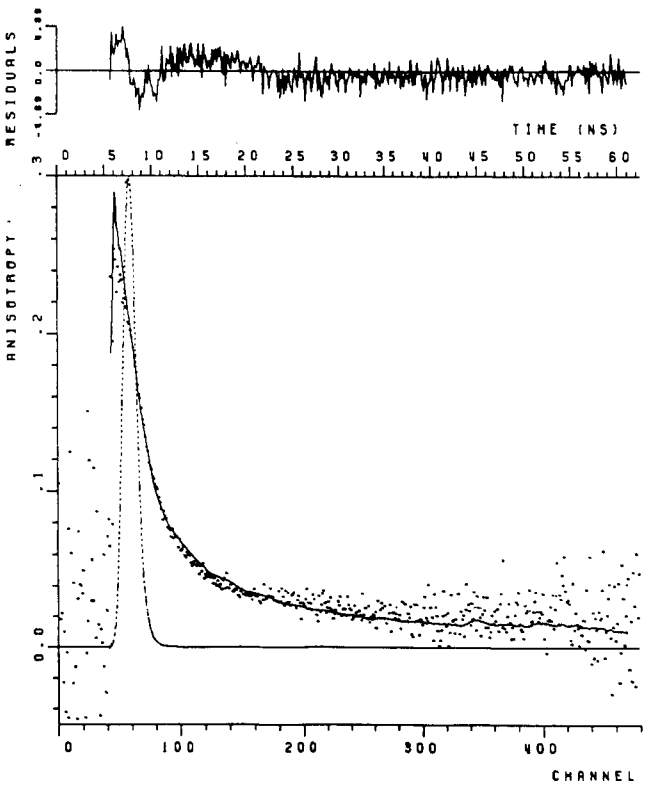

Figure 5. Comparison of Valeur, Jarry, Geny, and Monnerie's model to the experimental anisotropy at 62.7 °C.

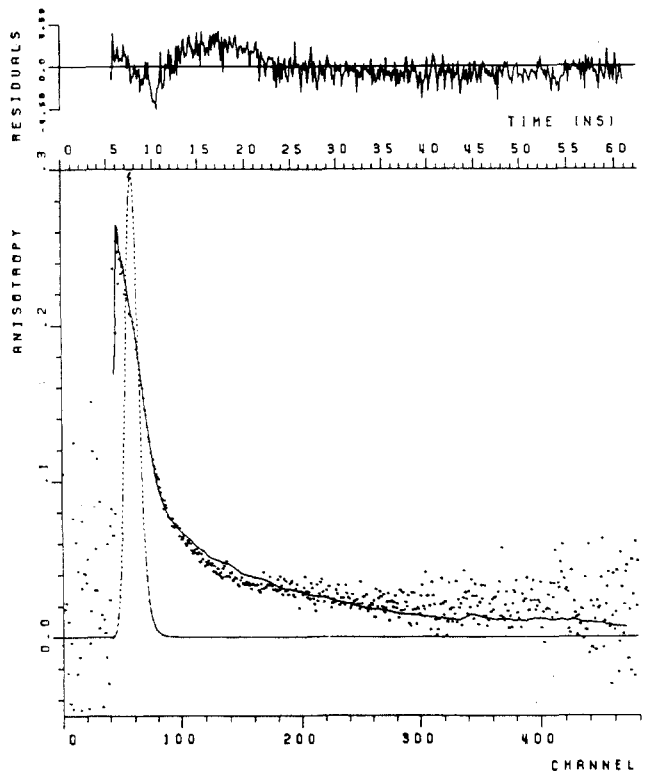

Figure 6. Comparison of Jones and Stockmayer's model to the experimental anisotropy at 62.7 °C.

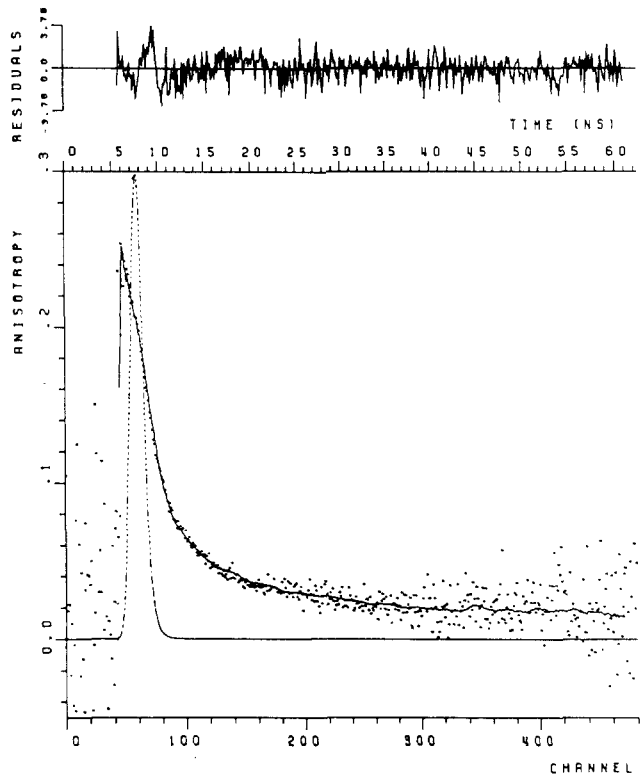

Figure 7. Comparison of Hall and Helfand's model to the experimental anisotropy at 62.7 °C.

the dotted line the excitation pulse (arbitrarily scaled). The weighted residuals are plotted above.

The restricted rotation[19] model is used only as a reference three-parameter expression. Its poor fit (Figure 3) is clearly visible by eye and emphasizes once more the very specific nonexponential character of polymer relaxation. But the rather poor fit obtained with the WW expression[13] is a much less common observation. In particular, it can be seen from Table III that the WW expression leads to very unstable best-fit parameters and unrealistic values for r_0. Even from a mere curve-fitting point of view, this expression is not as good as others, and it leads to higher values of χ^2 (compare Table III to Table V, or Figure 4 to Figure 7). Thus, this model, which appeared to account for the distribution of relaxation times observed in multimolecular experiments,[20-23] does not correspond to the shape of the OACF for one given vector of the chain. This is not so surprising. Indeed, if this OACF may formally be represented by a distribution of relaxation times, it arises from the one-dimension connectivity of the chain. The distribution of relaxation times observed, for instance, by dielectric relaxation in polymer melts cannot be associated only to this connectivity, since similar distributions are observed by this technique in nonpolymeric amorphous materials also. It probably contains other effects, such as the three-dimension correlation over different chains.

In spite of its better molecular basis, i.e., a one-dimension diffusion equation, the Valeur, Jarry, Geny, Monnerie (VJGM) model[1] also leads to relatively high values of χ^2 (Table III) which improve by short-time truncation. This is particularly sensitive at the lower temperatures (see, for instance, the results at 62.7 °C, Table III), where the initial behavior of the OACF is more precisely sampled. As previously observed for solutions[5] short-time truncation leads for the VJGM model to an unrealistic increase in r_0. This behavior is a consequence of the unphysical infinite slope at the origin arising from a continuous approximation in the treatment by Valeur and co-workers.[1]

This difficulty was overcome first by Jones and Stockmayer (JS) by keeping the diffusion equation in its discrete form.[2] This model leads to a series of two-parameter multiexponential expressions depending on the number of "bonds" taken into account in the computation. In contrast to what was observed for polystyrene in ethyl acetate–tripropionin solutions, where the "five-bond" expression fitted the data well, for PB in the melt the fit is improved by an increase in the number of "bonds" taken into account. But even with 13 bonds, the fit remains poor (see Table IV and Figure 6). Because of its discrete nature, the JS model does not sample continuously the space of possible OACF's. This introduces in the fitting a fortuitous character which cannot be avoided. Fortunately, the ideas underlying the JS model can be discussed in terms of more recent three-parameter expressions.

The three models presented in Table V lead to values of χ^2 and stabilities of parameters that are comparable and satisfying. From one experiment to another, one model or the other leads to a slightly better χ^2, but these fluctuations remain in the limits of what could be expected from statistical uncertainty, and no systematic trend could be assessed. It can be noticed that the weighted residuals show in the region of the excitation pulse a small discrepancy between the experimental curve and the best fit (see Figure 7). This discrepancy may betray residual spurious light, and the difficulty to perform very precise optical experiments in bulk polymers. Thus, as regards the criteria exposed above, and at the level of experimental precision, the three models are equivalent. As quoted in ref 5, the Bendler–Yaris (BY) model involves two arbitrary truncations in the distribution of modes of the one-dimension diffusion equation.[3] These truncations seem difficult to interpret directly in terms of molecular motions.

The expression of Hall and Helfand (Table II) actually corresponds to the conformation autocorrelation function (CCF) for a "chain of two-state elements" and has been recently derived.[4] It does not seem possible to derive

Table VI
Best-Fit Parameters Using Eq 5

θ, °C	χ^2	r_0	τ_1, ns	τ_2, ns	τ_2/τ_1	a
62.7	1.1786	0.241	1.44	34.95		−0.06
80.0	0.946 94	0.267	0.53	11.3	21	0.014

rigorously the orientation autocorrelation function from this CCF, but in the lack of a more rigorous treatment, Hall and Helfand[4] and Weber and Helfand[24] suggested that the expressions for the CCF should also describe reasonably well the OACF. In contrast to the VJGM one, this expression has a finite slope at the origin, and the fit to experimental data is improved (compare Table V to Table III), as it was for solutions.[5] The generalized diffusion and loss (GDL) expression is a semiempirical modification of the HH expression, suggested to us by the results of experiments performed on polystyrene in solution. In contrast to that previous study, the GDL expression does not lead to improved fitting in comparison to the HH one. For both, the ratio τ_2/τ_1, proportional to the ratio of the rate of the diffusive process to the loss rate, is higher than for polystyrene in ethyl acetate–tripropionine solutions.[5] But it is very similar to the values obtained in a separate experiment on PB in solution in toluene.[25] In that latter case, the ratio τ_2/τ_1 for the GDL and HH models remained in the range 25–35 in the temperature range explored, i.e., −60 to −5 °C. These experiments performed in dilute solution were also fitted by using the WW expression, leading to a β parameter close to 0.35 and values of χ^2 higher than these obtained by using the HH model. The first conclusion that can be drawn from the above comparison is that the models suitable to describe chain dynamics in solution can also be used to analyze the orientational motions in the melt. This is consistent with the idea that topological interchain effects act only on a large scale (entanglement distance) and do not change the local dynamic processes. This can be discussed more quantitatively by using four-parameter expressions. For instance, one can try to supplement the HH model by a residual anisotropy at long times due to anisotropic environment constraints:

$$r(t) = r_0\{(1 - a)\exp(-t/\tau_2 - t/\tau_1)I_0(t/\tau_1) + a\} \quad (5)$$

This expression improves only slightly χ^2 (Table VI) and the best-fit values of a are negative or positive depending on the temperature and on the data set. This reflects their lack of physical meaning. The variance–covariance matrix also reveals for relation 5 a variance for τ_2 much higher than for the original HH expression (see the example tabulated in Table VII) and a strong correlation between τ_2 and a. Thus, from a simple statistical point of view, the two parameters cannot be extracted independently from the data.

At the present level of experimental precision, the three-parameter HH or GDL expressions are sufficient to represent correctly the main-chain OACF in polymer melts. This observation is important for techniques like NMR or ESR, which require the a priori choice of a model to be interpreted. Of course, this agreement does not prove that the molecular processes invoked to build up the HH expression, i.e., correlated and isolated conformation jumps, are the real ones in polymer melts. As discussed elsewhere[5,25] the one-dimension diffusion equation can be associated with a variety of physical models, and the exponential asymptotic behavior seems to contradict rather well-established scaling laws.[26] But the agreement of the HH or GDL expression with our data demonstrates that the connectivity of the chain, which is responsible for the diffusive nature of the OACF, remains as essential in melts as it was in solution.

Effect of the Temperature. As quoted previously, when the temperature is decreased progressively below 50 °C, the fixed long-time limit of the experimental window hides an increasingly large part of the OACF. Thus, the experiment probes more and more local processes (more and more initial steps of the relaxation). Of course, it is still possible to fit a model to the observable part of the OACF, but one must keep in mind that, in this temperature domain, FAD can suffer from the same artifacts as techniques which perform discrete sampling (NMR, etc.). Important results like the temperature evolution of parameters can become model dependent. (The remaining advantage of FAD in that case is that one can check by direct visual observation of the experimental anisotropy if the OACF is correctly sampled or not.)

The best-fit parameters for the HH model at different temperatures are gathered in Table VIII. As far as could be measured the ratio τ_2/τ_1 remained rather high so that the τ_2 term (loss term) was weighted worse and worse when the temperature was lowered. Indeed, a stable and significant fit of τ_2 with the HH expression was possible above 40 °C only. From a physical point of view these high values of τ_2/τ_1 imply that the processes responsible for the loss (whatever their molecular nature is) are very rare. Most of the motions responsible for orientation decorrelation are correlated along the chain. Indeed, neglecting the loss term (i.e., putting arbitrarily $1/\tau_2$ equal to 0) increases χ^2 only slightly, and a rather satisfactory fit can be obtained by using the diffusive term only.

As already observed for PS in solution[5] the GDL expression seems to lead to a different weighting of the diffusive and loss term and to allow a more stable fit of τ_2; thus, we have been able to use it down to lower temperatures than the HH one. This property makes the GDL expression a convenient curve-fitting one to study more quantitatively the evolution of the OACF as a function of

Table VII
Variance–Covariance Matrices for the HH Model and Expression 5

	variance–covariance matrix				
	r_0	τ_1	τ_2	a	rel SD[a]
		HH Model			
r_0	1.1×10^{-5}	3.5×10^{-5}	-4.2×10^{-5}		0.003
1	3.5×10^{-5}	1.7×10^{-4}	-2.1×10^{-4}		0.01
2	-4.2×10^{-5}	-2.1×10^{-4}			0.02
		Relation 5			
r_0	2.5×10^{-5}	8.0×10^{-5}	2.2×10^{-4}	-1.1×10^{-4}	0.005
1	8.0×10^{-5}	3.2×10^{-4}	2.8×10^{-3}	-7.0×10^{-4}	0.02
2	2.2×10^{-4}	2.8×10^{-3}	0.50	-3.9×10^{-2}	0.7
a	-1.1×10^{-4}	-7.0×10^{-4}	-3.9×10^{-2}	4.3×10^{-3}	0.07

[a] Relative standard deviation.

Table VIII
Temperature Evolution of the Best-Fit Parameters for Models GDL and HH

θ, °C	model	χ^2	r_0	τ_1, ns	τ_2, ns	τ_2/τ_1
-33.9	GDL	1.563	0.313	223	(1×10^3)	
-19.5	GDL	1.556	0.303	57.9	(4×10^3)	
-11.4	GDL	1.378	0.297	31.6	(5×10^3)	
-0.9	GDL	1.318	0.293	19.8	565	28
8.4	GDL	1.335	0.292	11.4	221	19
	HH	1.344	0.289	22.2	(3×10^6)	
22.0	GDL	1.212	0.258	5.64	164	29
30.0	GDL	1.451	0.280	3.24	82	25
	HH	1.560	0.275	6.98	(9×10^3)	
40.9	GDL	1.455	0.284	1.84	44	24
	HH	1.687	0.286	4.54	95	21
50.0	GDL	1.406	0.254	1.39	45	32
	HH	1.204	0.241	3.62	110	31
62.7	GDL	1.176	0.251	0.75	36	48
	HH	1.248	0.234	2.22	97	43
80.0	GDL	0.978	0.268	0.33	12	36
	HH	0.962	0.246	1.01	22	22

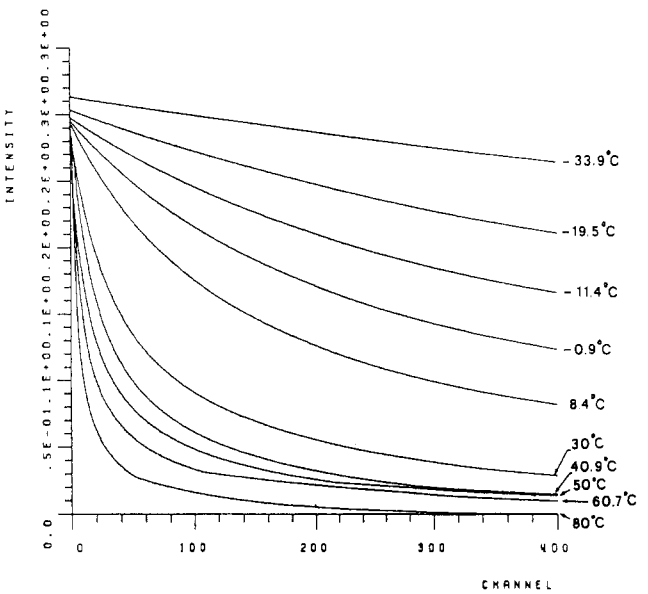

Figure 8. Temperature evolution of the best-fit OACF (GDL model).

the temperature. As can be seen in Figure 8, the evolution of the best-fit OACF's (GDL model) as a function of temperature is rather continuous. The evolution of τ_1 and τ_2 is given in an Arrhenius plot (Figure 9). The values of τ_1 for each model are correctly fitted by two parallel straight lines, with no special perturbation in the domain where truncation artifacts should appear (20–40 °C). This was also true for the BY model, not represented. The longer time τ_2 could be determined approximately only in the range 20–80 °C and with the GDL model. In this domain, its behavior seems similar to that of τ_1. So, whatever the physical origin of the τ_2 term is, its behavior indicates that the shape of the OACF remains more or less unchanged when the temperature is varied.

The relaxation of the chain in this temperature range probably does not involve several processes of very different activation energies.

The apparent activation energy, 39 ± 4 kJ/mol, agrees fairly well with the slope of the α relaxation (or "high-frequency glass transition") in this temperature range given by the WLF parameters of polybutadiene deduced from mechanical relaxation experiments[26] (dotted line, arbitrarily shifted). Thus, the main processes of orientation relaxation are involved in the global activation which also

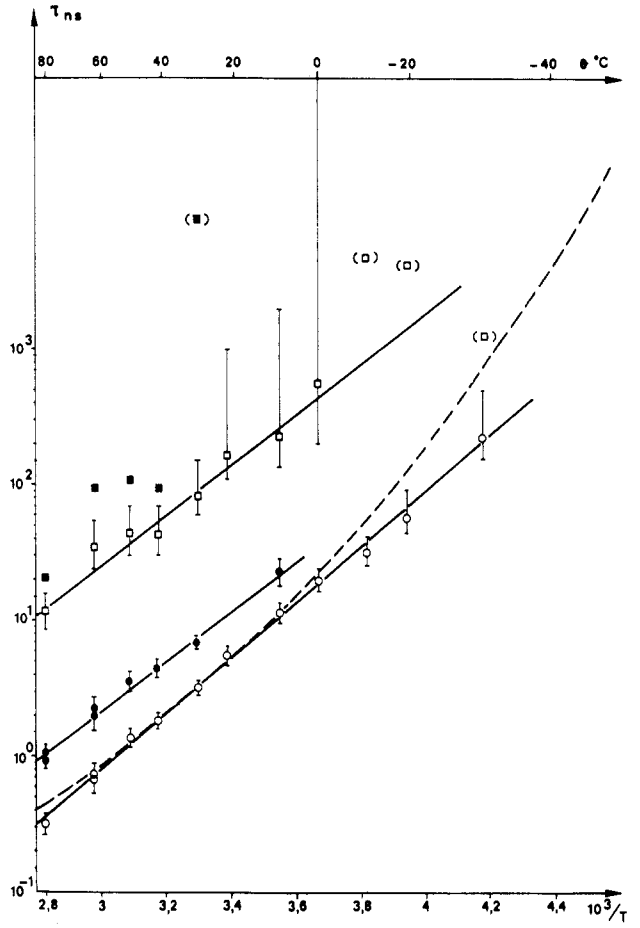

Figure 9. Arrhenius plot of the best-fit relaxation times; HH model, τ_1 (●) and τ_2 (■); GDL model, τ_1 (○) and τ_2 (□); the dashed line corresponds to the WLF relation (ref 26).

drives mechanical relaxation. It is noteworthy that the experimental curve seems more linear than the WLF one. As a matter of fact, at very low temperatures, only the initial slope of the OACF is probed (see Figure 8). This initial slope may, for instance, reflect mainly an oscillation of small amplitude, not involved in the critical slowing down of the medium.

Conclusions

In a suitable temperature range fluorescence anisotropy decay can be used to study the main orientational relaxation processes in polymer melts, i.e., processes which relax the orientation autocorrelation function from, say, 0.95 to 0.05.

In the case of polybutadiene, the orientation relaxation of the skeleton has the same temperature evolution as the mechanical properties. This supports the idea that macroscopic properties such as the glass transition results from an accumulation of local molecular processes.

The shape of the orientation autocorrelation function is strikingly similar to the shape observed in dilute solution. This leads one to expect that, in most cases, models originally proposed for polymers in solution, like the recent model by Hall and Helfand,[4] can be used to analyze orientational dynamic experiments performed on polymer melts. This shape, characteristic of a one-dimensional diffusion-and-loss process, shows that the connectivity of the chain remains an essential element of melt dynamics. But the molecular nature of the processes responsible for the principal main-chain orientation relaxation is still not clearly elucidated. The present study suggests that their scale remains rather small since they do not seem to be

affected by entanglements. Another approach to these questions will be proposed in the next paper of this series, using probes with short chains of variable length.

Acknowledgment. We acknowledge with gratitude the technical support of Les Etablissements Michelin.

References and Notes

(1) B. Valeur, J. P. Jarry, F. Geny, and L. Monnerie, *J. Polym. Sci., Polym. Phys. Ed.*, **13**, 667, 675 (1975).
(2) A. A. Jones and W. H. Stockmayer, *J. Polym. Sci., Polym. Phys. Ed.*, **15**, 847 (1975).
(3) J. T. Bendler and R. Yaris, *Macromolecules*, **11**, 650 (1978).
(4) C. K. Hall and E. Helfand, *J. Chem. Phys.*, **77**, 3275 (1982).
(5) J. L. Viovy, L. Monnerie, and J. C. Brochon, *Macromolecules*, **16**, 1845 (1983).
(6) See, for instance, J. D. Ferry, "Viscoelastic Properties of Polymers", 2nd ed., Wiley, New York, 1970.
(7) See, for instance, "Dielectric Properties of Polymers", F. E. Karasz, Ed., Plenum Press, London, 1972.
(8) H. W. Spiess, *J. Chem. Phys.*, **72**, 6755 (1980).
(9) P. Lindner, E. Rossler, and H. Sillescu, *Makromol. Chem.*, **182**, 8653 (1981).
(10) O. W. Howarth, *J. Chem. Soc., Faraday Trans. 2*, **76**, 1219 (1980).
(11) See, for instance, P. Törmala, *J. Macromol. Sci., Rev. Macromol. Chem.*, **C17**, 197–357 (1979).
(12) J. P. Jarry and L. Monnerie, *J. Polym. Sci., Polym. Phys. Ed.*, **16**, 443 (1978); 18, 1879 (1980).
(13) G. Williams and D. C. Watts, *Trans. Faraday Soc.*, **66**, 80 (1971).
(14) B. Valeur and L. Monnerie, *J. Polym. Sci., Polym. Phys. Ed.*, **14**, 11, 29 (1976).
(15) J. C. Brochon in "Protein Dynamics and Energy Transduction", Shin'ishi Ishiwata, Ed., Taniguchi Foundation, Japan, 1980.
(16) P. R. Bevington, "Data Reduction and Error Analysis for the Physical Sciences", McGraw-Hill, New York, 1969.
(17) D. M. Rayner, A. E. McKinnon, A. G. Szabo, and P. A. Hacket, *Can. J. Chem.*, **54**, 3246 (1976).
(18) J. Durbin and G. S. Watson, *Biometrika*, **37**, 409 (1950); **38**, 159 (1951).
(19) K. Kinosita, S. Kawato, and A. Ikegamai, *Biophys. J.*, **20**, 289 (1977).
(20) G. Williams, *Adv. Polym. Sci.*, **33**, 59 (1979).
(21) G. D. Patterson, C. P. Lindsey, and J. R. Stevens, *J. Chem. Phys.* **70**, 643 (1979).
(22) G. D. Patterson and C. P. Lindsey, *Macromolecules*, **14**, 83 (1981).
(23) G. D. Patterson, *Adv. Polym. Sci.*, **48**, 125 (1983).
(24) T. A. Weber and E. Helfand, *J. Phys. Chem.*, **87**, 2881 (1983).
(25) J. L. Viovy, Thèse, Université Pierre et Marie Curie, Paris, 1983.
(26) An exponential decay of the orientation autocorrelation function at long time would lead to a monomer translation diffusion coefficient which tends toward infinity when the length of the chain increases. Thus, the exponential behavior should cross over somewhere to a $t^{-1/2}$ behavior in order to be consistent with the Rouse regime (P. G. De Gennes, *Physics*, (*Long Island City, N.Y.*) **3**, 37 (1967)).

Effect of Main-Chain Double Bond on Dynamics of Polystyrene: An ESR Study of Macromolecules Spin Labeled by Copolymerization

Pál Simon,* László Sümegi, Antal Rockenbauer, and Ferenc Tüdös

Central Research Institute for Chemistry, Hungarian Academy of Sciences, H-1525 Budapest, Hungary

József Csekö and Kálmán Hideg

Central Laboratory, Chemistry, University Pécs, H-7643 Pécs, Hungary.
Received April 13, 1984

ABSTRACT: ESR relaxation measurements were carried out for a dilute toluene solution of in-chain-labeled polystyrene containing double bond in the main chain next to the spin label. The temperature was varied from −20 to +93 °C. It was found that the correlation time is larger by an order of magnitude than that of the unlabeled polystyrene, which can be explained by the influence of double bond on the segmental motion. The number of monomer units involved in the ESR relaxation process was estimated as 2–4. The preparation of spin-labeled polystyrene copolymer was also described.

Introduction

ESR spectroscopy is a useful technique for investigating the dynamics of spin-labeled macromolecules, in the present work, polystyrene. The labels can be covalently bound to different parts of the polystyrene: at the end of the chain, in the side chain, or within the chain. Friedrich et al. have reviewed the intramolecular motion of polystyrene in dilute solution.[1] The measurements have clearly demonstrated the segmental character of motion involved in the relaxation process since the correlation time was found to be independent of the molecular weight above 10 000.

Correlation times of polystyrene samples spin labeled within the chain (τ_c(317 K) = 1.6×10^{-10} s)[1] and in the side chain (τ_c(317 K) = 3.5×10^{-10} s)[2] respectively coincide with that of the segmental motion of unlabeled polystyrene (τ_c(317 K) = 2×10^{-10} to 6×10^{-10} s, studied by ^{13}C NMR).[3-5] This indicates that the correlation time of the spin label is mainly affected by the segmental motion of the polystyrene chain and is not altered significantly by the conformational changes of the label itself. Consequently, the correlation time measured in polystyrene samples reflects the local motion of segments in the vicinity of labels in the polymer chain.

The aim of this paper is to investigate the effect of main-chain double bond on the local segmental motion of polystyrene in dilute solution via monitoring the correlation time of rotational diffusion motion of a special spin label. A double bond in the polymer backbone can hinder the motion of segments in its vicinity and alter the correlation time with respect to the unlabeled polystyrene. In order to carry out experiments we have synthesized a

0024-9297/85/2218-1137$01.50/0